Electronic Supplementary Information (ESI) for Journal of Materials Chemistry B
This journal is©The Royal Society of Chemistry 2019

Electronic Supplementary Information for:

Polydopamine-Coated Laponite®-Stabilized Iron Oxide Nanoplatform for Targeted Multimodal Imaging-Guided Photothermal Cancer Therapy

Mengxue Liu [a], Jiulong Zhang [b], Xin Li [a], Chao Cai a, Xueyan Cao [a], Xiangyang Shi [a] *, Rui Guo [a] *

[a] State Key Laboratory of Modification of Chemical Fibers and Polymer Materials, College of Chemistry, Chemical Engineering and Biotechnology, Donghua University, Shanghai 201620, People's Republic China

[b] Department of Radiology, Shanghai Public Health Clinical Center, Fudan University Shanghai 201508, People's Republic China

Part of experimental section

Characterization techniques

^{1}H NMR spectra were measured on a Bruker AV400 NMR spectrometer. Samples were dissolved in D_2O before measurement. The FTIR spectra were acquired using a Nicolet Nexus 670 FTIR (Nicolet-Thermo) spectrometer. The spectra of all samples were recorded in a transmission mode with the wavenumbers in the range of 400–4000 cm^{-1}. UV-Vis spectroscopy was obtained using a Lambda 25 UV-Vis spectrophotometer (Perkin-Elmer, USA). The crystalline structures of LAP, Fe_3O_4, LAP-Fe_3O_4 were characterized by a Rigaku D/max-2550 PC X-ray diffraction (XRD) system (Rigaku Co., Tokyo, Japan) equipped with Cu Kα radiation (λ = 0.154 nm) at 40 kV and 200 mA. The scan was performed from 5° to 60° (2θ). Zeta potential and dynamic light scattering (DLS) measurements were carried out using a Malvern Zeta-sizer Nano ZS model ZEN3600 (Worcestershire, U.K.) equipped with a standard 633 nm laser. Before performing the measurements, the samples were dispersed in water at concentration of 0.1 mg mL^{-1}. The organic component of the samples was quantified by thermo gravimetric analysis (TGA) using a TG 209 F1 (NETZSCH Instruments Co, Ltd., Selb/Bavaria, Germany). The samples were heated from 25°C to 900°C at a rate of 10°C/min under nitrogen atmosphere. Transmission electron microscopy (TEM) was carried out with a JEOL 2010 analytical electron microscope (Tokyo, Japan) operating at 200 kV to characterize the morphology and size of the NPs. Before performing the measurements, the samples were prepared by putting a drop of diluted suspension (6 μL) onto a carbon-coated copper grid and dried in air. For each sample, at least 100 particles in different TEM images were randomly selected and measured and use Image J software to calculate the size distribution of the NPs. The Fe concentrations of samples were analyzed by using a Lee man Prodigy ICP-OES system (Hudson, NH).

Photothermal conversion Temperature elevation induced by NIR laser irradiation

300 μL of LAP, Fe_3O_4, PDA, LAP-Fe_3O_4, LAP-Fe_3O_4@PDA, LAP-Fe_3O_4@PDA-mPEG and LAP-Fe_3O_4@PDA-PEG-PBA solutions were irradiated by an NIR laser (Shanghai Xilong Optoelectronics Technology Co. Ltd., Shanghai, China) (808 nm, 1.2 W/cm^2) for 5 min. The temperature was recorded every 5 s by an online DT-8891 Ethermo couple thermometer (STPC-510P, Xiamen Baidewo Technology Co., China). In order to investigate the photothermal stability, five cycles of repeated laser irradiation were applied to LAP-Fe_3O_4@PDA-PEG-PBA solution. For each cycle, the solution was heated by an 808 nm laser irradiation (0.25 cm^2, 1.2 W/cm^2, 5 min) and followed by a cooling period to room temperature. The solution temperature was recorded every 5 s by thermometer.

ROS Production

1,4-diphenyl-2,3-benzofuran (DPBF) was used as a ROS chemical probe to evaluate the $^1O_2$ generation capability of LAP-Fe_3O_4@PDA-PEG-PBA. Specifically, 2 mL of a DPBF/DMF solution (20 μM) was added to 2 mL of PBS, LAP, LAP-Fe_3O_4, PDA-PEG-PBA and LAP-Fe_3O_4@PDA-PEG-PBA aqueous solution, respectively. Each mixture was irradiated by an 808 nm laser (1.2 W/cm^2) for 8 min. Then the absorption intensity of DPBF in different solutions at 417 nm was evaluated by UV-vis spectroscopy.

MR and PA Imaging of LAP-Fe_3O_4@PDA-PEG-PBA solution

LAP-Fe_3O_4@PDA-PEG-PBA and LAP-Fe_3O_4@PDA-mPEG solutions with different Fe concentrations (0.005, 0.01, 0.02, 0.04

and 0.08 mM) in 2 mL Eppendorf tubes were scanned by a 3.0 T SIEMENS MAGNE TOM VERIO clinical MR system. The instrumental parameters were set at point resolution of 156 mm × 156 mm, section thickness of 0.6 mm, TR of 5800 ms, TE of 100 ms, and number of excitation =1. Dimensional (2D) spin-echo T_2-weighted MR images and linear fitting of $1/T_2$ (r_2 relaxation rate) of LAP-Fe_3O_4@PDA-mPEG and LAP-Fe_3O_4@PDA-PEG-PBA with different Fe concentrations (0.005, 0.01, 0.02, 0.04, and 0.08 mM) were obtained. The transverse relaxivity of NPs was calculated by a linear fitting of the inverse T_2 ($1/T_2$) relaxation time as a function of Fe concentration (mM).

The LAP-Fe_3O_4@PDA-PEG-PBA and LAP-Fe_3O_4@PDA-mPEG solutions with different Fe concentrations (62.5−500 μg/mL) were injected into the thin hose which was buried in an ultrasonic special glue and then irradiated under an 875 nm laser. The PA images were measured using the Vevo LAZR PA Imaging System (Visualsonics Inc., Toronto, Canada). The intensity of PA signal was evaluated in arbitrary units (a.u.) by selecting a region of interest in the digital PA images.

In vitro assays

SA-overexpressed mouse breast cancer 4T1 cells were seeded into 96-well plates at a density of 1×10^4 cells/well and incubated at 37°C in 5% CO_2 atmosphere for 24 h. Then the medium was replaced by fresh medium containing PBS, LAP-Fe_3O_4@PDA-mPEG or LAP-Fe_3O_4@PDA-PEG-PBA (at the same Fe concentrations ranging from 50 to 150 μg/mL) for 24 h. The medium was replaced by addition of 100 μL fresh DMEM containing 10 μL CCK-8 and incubated for another 3 h. The absorbance was measured by Thermo Scientific Multiskan MK3 ELISA reader (Thermo Scientific, Hudson, NH) at 450 nm in each well. For PTT treatment group, the cells were irradiated by an 808 nm laser (1.2 W/cm^2) for 5 min after washed with saline for 3 time. In addition, the cells were stained by the live/dead viability assay. The dead cells were stained with PI solution (8 μM) and live cells with AM solution (2 μM) at the room temperature for 15-30 min, washed with PBS for 3 times. Finally, the cells were observed via a fluorescence microscopy (CARL Zeiss, Axio Vert. A1, Germany).

To confirm the uptake of LAP-Fe_3O_4@PDA-PEG-PBA and LAP-Fe_3O_4@PDA-mPEG NPs, 4T1 cells were cultured in a 12-well plate at a density of 2×10^5 cells per well for one day prior to the experiment. Then the cell culture medium was replaced with 1 mL fresh medium containing PBS (control), LAP-Fe_3O_4@PDA-PEG-PBA and LAP-Fe_3O_4@PDA-mPEG NPs at different Fe concentrations (0.05 and 0.1 μg/mL) and the cells were incubated for 4 h at 37 °C and 5% CO_2. The cells were then washed with PBS for 3 times, and fixed with 2.5% of glutaraldehyde in PBS for 15 min at 4 °C. After that, the cells were rinsed 3 times with PBS and 1 mL of Perls stain (Perls stain A1/Perls stain A2, v/v = 1 : 1) was added, followed by keeping it still at 37 °C in the dark for 30 min. Then the cells were quickly washed 3 times with PBS in 30 s and observed by light microscopy (Leica DM IL LED inverted phase contrast microscope) with a magnification of 200× for each sample. Similar to the protocol described above, 4T1 cells were treated with LAP-Fe_3O_4@PDA-PEG-PBA and LAP-Fe_3O_4@PDA-mPEG NPs NPs with Fe concentrations ranging from 50 to 150 μg/mL. After 4 h, the cells were washed with PBS 3 times, trypsinized, resuspended, counted and lysed using an aqua regia solution (nitric acid/hydrochloric acid, v/v = 3 : 1). The cellular uptake of the Fe element was measured by ICP-OES.

In vivo MR/PA imaging and biodistribution after intravenous injection

We performed animal experiments following the protocols approved by the institutional committee for animal care, in accordance with the policy of the National Ministry of Health. Famale 5-week-old BALB/c nude mice (15-20 g, Shanghai Slac Laboratory Animal Center, Shanghai, China) were subcutaneously injected with 2×10^6 4T1 cells per mouse on the right back. When the size of tumor reached a volume of 0.08−0.1 cm^3, the mice were anesthetized by intraperitoneal injection of pentobarbital sodium (40 mg kg^{-1}), and then intravenously injected with LAP-Fe_3O_4@PDA-mPEG or LAP-Fe_3O_4@PDA-PEG-PBA solutions (Fe=[300 μg/mL], one mouse per group). MR scanning was performed using a 3.0 T SIEMENS MAGNE TOM VERIO clinical MR system with the same parameters as those used for in nanoparticles MR imaging. For each animal, dimensional (2D) spin-echo T_2-weighted MR images were obtained before injection and at 10, 20, 30, 40, 50, 60 min postinjection.

For PA imaging, LAP-Fe_3O_4@PDA-mPEG or LAP-Fe_3O_4@PDA-PEG-PBA NPs were dispersed in PBS (0.1 mL PBS, 50 μg Fe per mouse) and injected to each mouse via the tail vein. The image of the tumor site was scanned (0, 10, 20, 30, 40, 50 and 60 min, respectively) post intravenous injection by Vevo LAZR photoacoustic imaging system equipped with an 875 nm laser (Visual Sonics Inc., Toronto, Canada). The tumor-bearing mice after MR and PA scanning were euthanized at different time (40 min, 24 h and 96 h) post-injection and the heart, liver, spleen, lung, kidney, and tumor were extracted and weighed. The organs were then cut into 1-2 mm^2 pieces and digested by aqua regia solution (nitric acid/hydrochloric acid, v/v = 1:3) for 24 h. Then, the Fe content in the pieces of different organs was quantified by ICP-OES. For comparison, the mice injected with PBS were used as control.

In Vivo PTT and thermal/PA imaging after intratumoral injection

The 4T1 tumor-bearing nude mice with tumor volume of 0.05−0.06 cm^3 were assigned to 6 groups (n=5): Group 1 (PBS); Group 2 (PBS + Laser); Group 3 (LAP-Fe_3O_4@PDA-mPEG, Non-targeted); Group 4 (LAP-Fe_3O_4@PDA-PEG-PBA, Targeted); Group 5 (Non-targeted + Laser); and Group 6 (Targeted + Laser). Non-targeted and Targeted materials with the same Fe concentration (0.1 mL PBS, 30 μg Fe per mouse) were intratumorally injected on Day 1 and Day 10, and 10 min after administration, mice were irradiated with 808 nm NIR laser at a power of 1.2 W/cm^2 for 5 min. The tumor volume and body weight of all mice were recorded every other day, and the pictures of mice were taken by digital camera. For in vivo imaging, 0.1 mL of PBS was intratumorally

injected as a control. The thermal images were recorded by FLIR A300 photothermal medical device (IRS Systems Inc., Shanghai, China) coupled with an infrared camera. For PA imaging, LAP-Fe_3O_4@PDA-mPEG or LAP-Fe_3O_4@PDA-PEG-PBA NPs were dispersed in PBS (0.1 mL PBS, 30 μg Fe per mouse) and intratumoral injected to each mouse. The image of the tumor site was scanned (control, 0.5 h, 4 h and 8 h, respectively) post injection by Vevo LAZR photoacoustic imaging system equipped with an 875 nm laser (Visual Sonics Inc., Toronto, Canada).

Histology examinations

Tumor cell apoptosis efficacy was evaluated on tumor tissues using a terminal deoxynucleotidyl transferase dUTP nick end labeling (TUNEL) method through the use of in situ apoptotic detection kit (KeyGEN BioTECH, Nanjing, China) according to the manufacturer's guidelines. Briefly, after photothermal treatment, the tumor of the mice was harvested, fixed in paraformaldehyde, dehydrated, paraffin-embedded, and finally sectioned. The section was then deparaffinized, rehydrated, washed, stained using a TUNEL Kit, and also examined with a Leica DM IL LED inverted phase contrast microscope. The number and percentage of TUNEL-positive cells were counted from five random selected fields per section. To identify the reason of mortality, the lung was harvested when the mice died after different treatments. Then the lungs were fixed with 10% neutral buffered formalin, embedded in paraffin, sectioned into slices with a thickness of 4 mm, stained with hematoxylin and eosin (H&E) using a typical procedure, and observed using a Leica DM IL LED inverted phase contrast microscope with a magnification of 200×.

To evaluate the toxicity of materials, health mice treated with saline group, LAP-Fe_3O_4@PDA-mPEG and LAP-Fe_3O_4@PDA-PEG-PBA (0.2 mL PBS, 60 μg Fe per mouse) for 15 days were euthanized. Then, the major organs including heart, liver, spleen, and kidney were harvested for H&E staining and being photographed.

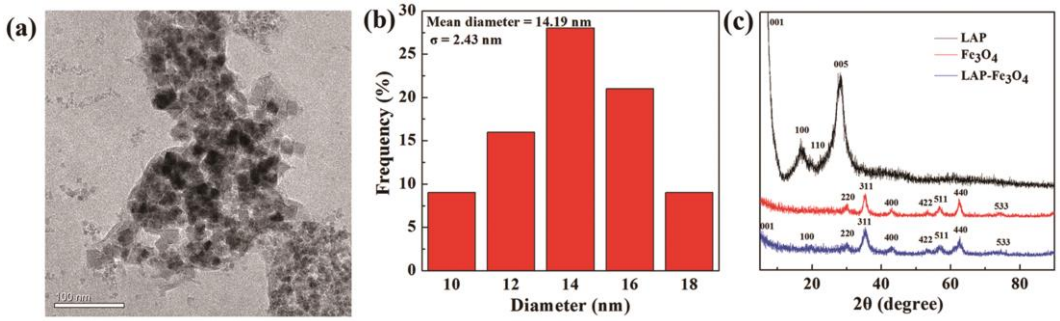

Fig. S1 (a) TEM image and (b) size distribution histogram of LAP-Fe_3O_4 NPs; (c) XRD patterns of LAP, Fe_3O_4 and LAP-Fe_3O_4 NPs.

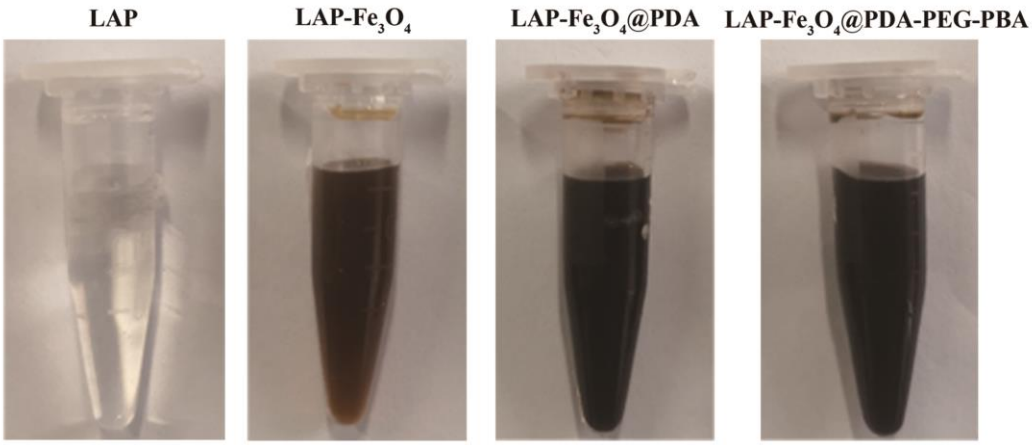

Fig. S2 Photos of LAP, LAP-Fe_3O_4, LAP-Fe_3O_4@PDA and LAP-Fe_3O_4@PDA-PEG-PBA solutions.

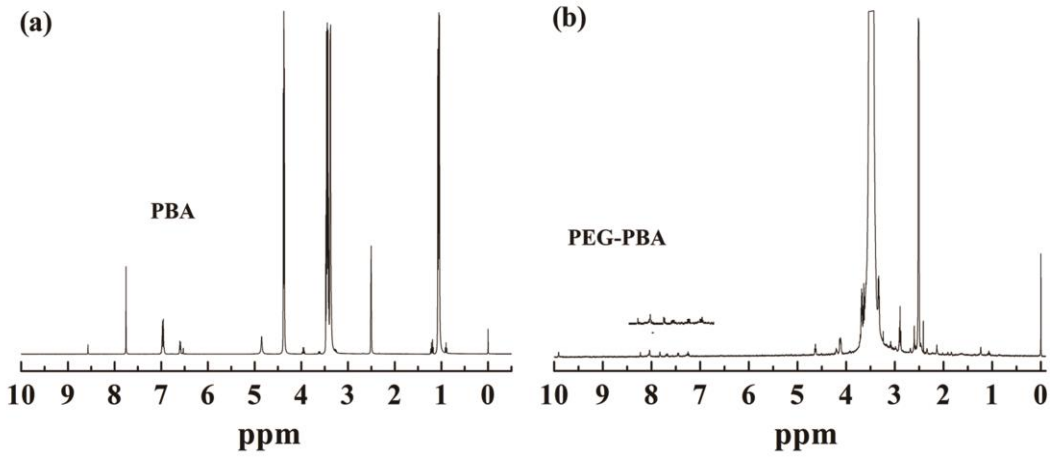

Fig. S3 ^{1}H NMR spectra of (a) PBA and (b) PEG-PBA.

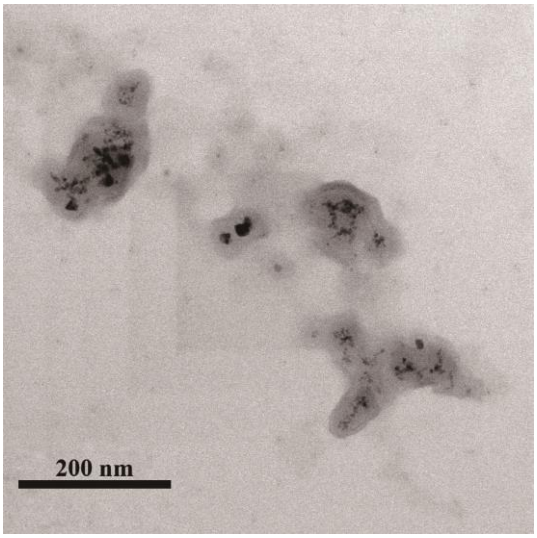

Fig. S4 TEM image of LAP-Fe_3O_4@PDA-PEG-PBA NPs in field of 200 nm view.

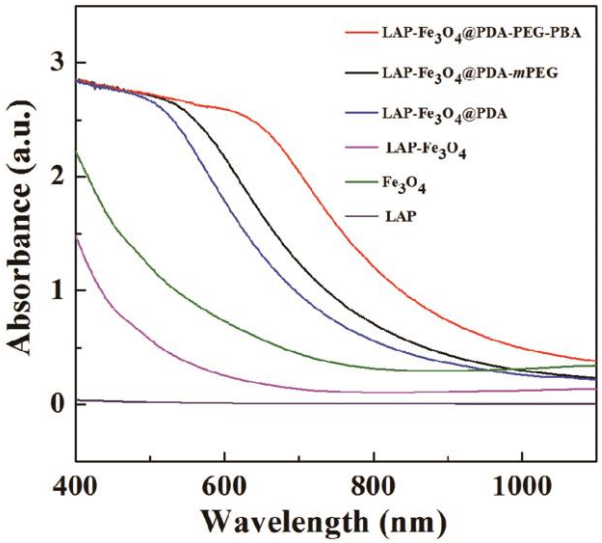

Fig. S5 UV-vis spectra of LAP, Fe_3O_4, LAP-Fe_3O_4, LAP-Fe_3O_4@PDA, LAP-Fe_3O_4@PDA-mPEG and LAP-Fe_3O_4@PDA-PEG-PBA.

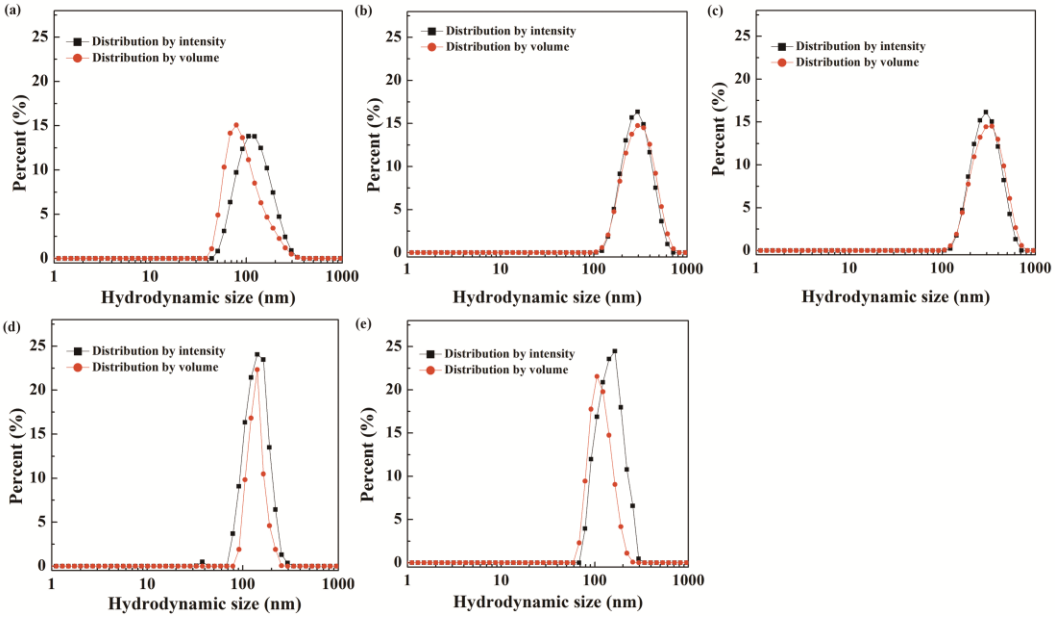

Fig.S6 Hydrodynamic size distributions of the (a) Fe_3O_4 NPs, (b) LAP-Fe_3O_4, (c) LAP- Fe_3O_4@PDA, (d) LAP-Fe_3O_4@PDA-*m*PEG and (e) LAP-Fe_3O_4@PDA-PEG-PBA NPs measured by intensity and volume, respectively.

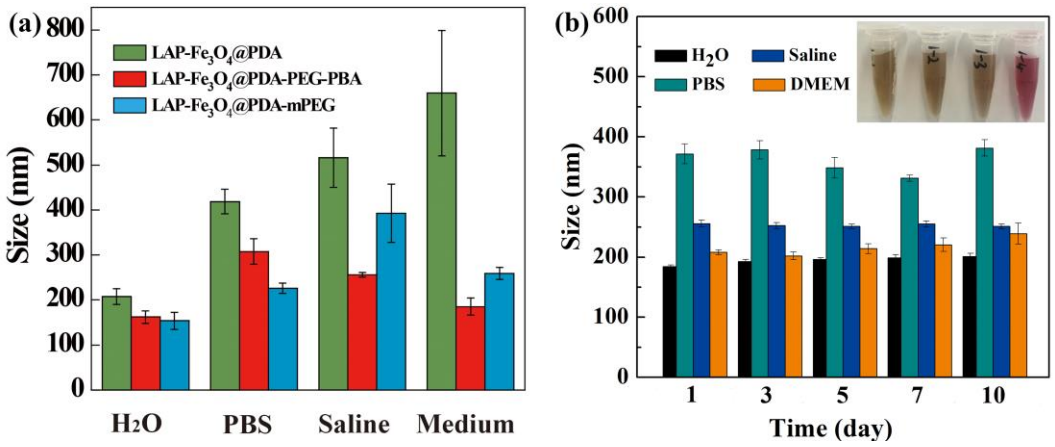

Fig. S7 The hydrodynamic size of (a) LAP-Fe_3O_4@PDA, LAP-Fe_3O_4@PDA-*m*PEG and LAP-Fe_3O_4@PDA-PEG-PBA in different solvents and (b) LAP-Fe_3O_4@PDA-PEG-PBA NPs in different solvents for 1, 3, 5, 7 and 10 days (Images of LAP-Fe_3O_4@PDA-PEG-PBA dispersed in water, PBS, Saline and Medium from left to right).

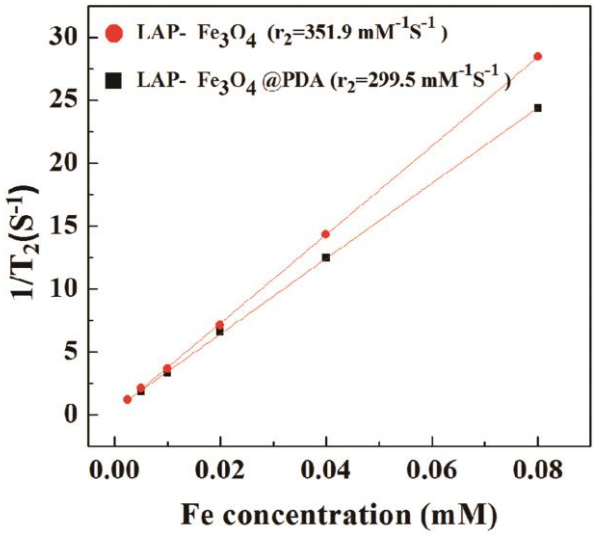

Fig.S8 T_2-weighted MR linear fitting of r_2 relaxation rate ($1/T_2$) of LAP-Fe_3O_4 and LAP-Fe_3O_4@PDA at different Fe concentrations (0.005, 0.01, 0.02, 0.04, and 0.08 mM).

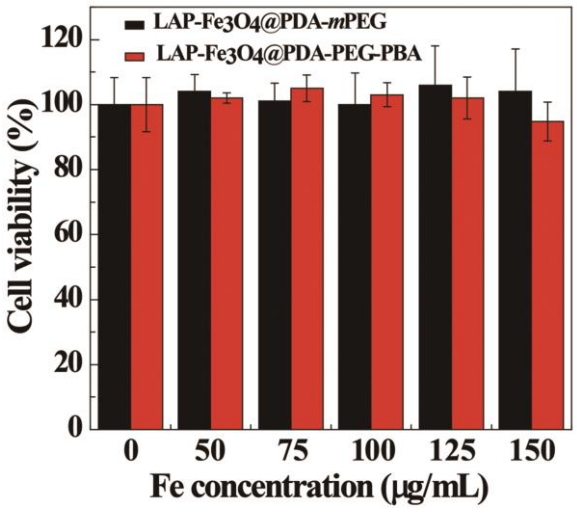

Fig. S9 CCK-8 viability assay of 4T1 cells treated with LAP-Fe_3O_4@PDA-mPEG and LAP-Fe_3O_4@PDA-PEG-PBA at different Fe concentrations ([Fe]=50, 75, 100, 125 and 150 μg/mL) for 24 h, respectively.

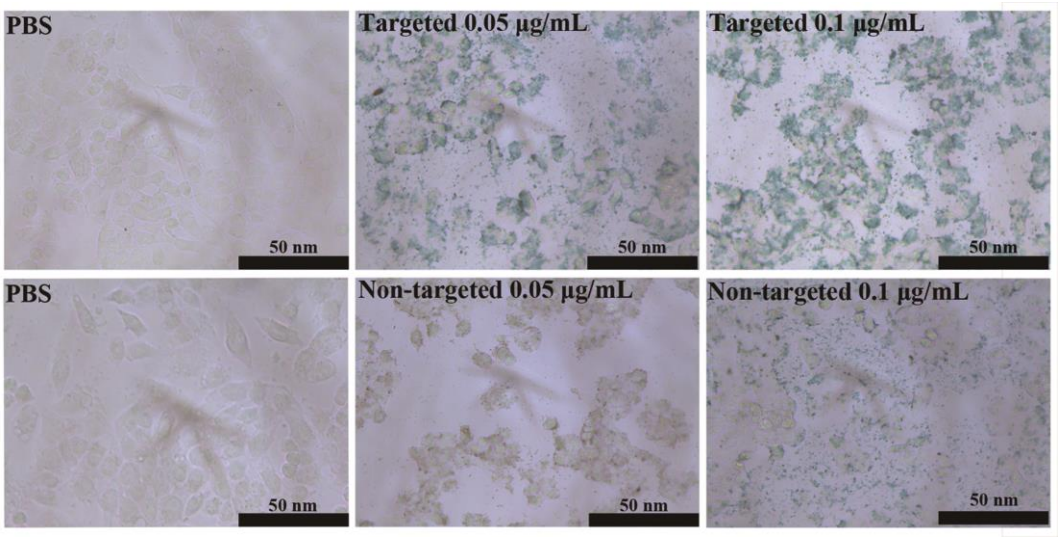

Fig. S10 Prussian blue staining micrographs of 4T1 cells treated with PBS, Targeted and Non-targeted NPs at different Fe concentrations for 4 h.

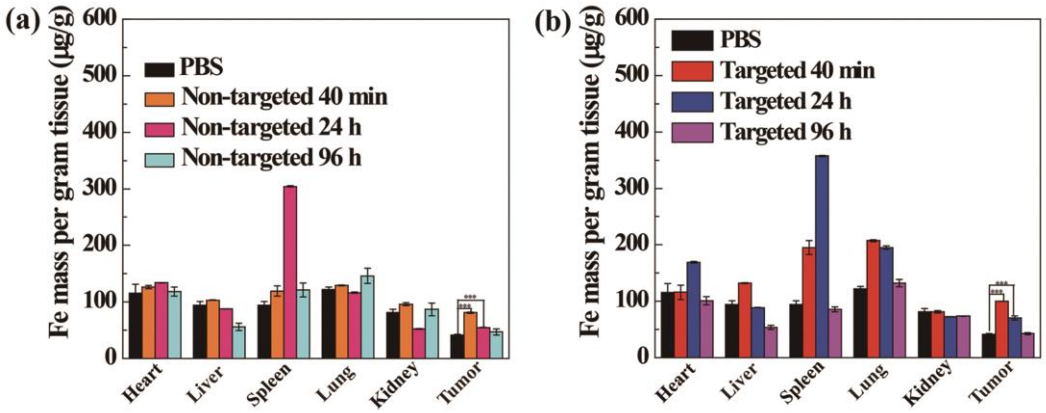

Fig. S11 In vivo biodistribution of Fe content in the major organs of the mice including heart, liver, spleen, lung, kidney, and tumor at different time post intravenous injection of (a) Non-targeted NPs and (b) Targeted NPs ([Fe]=300 μg mL^{-1}, 0.2 mL PBS).

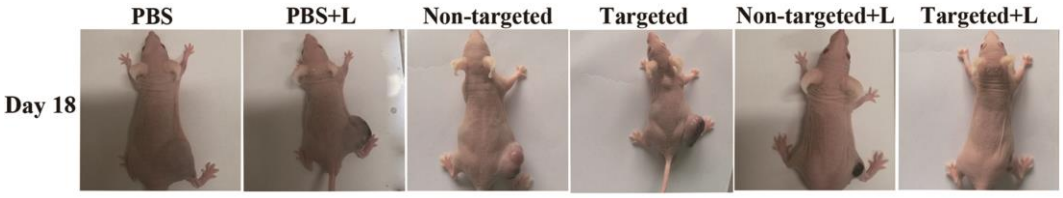

Fig. S12 The photographs of mice on day 18 after different treatments.

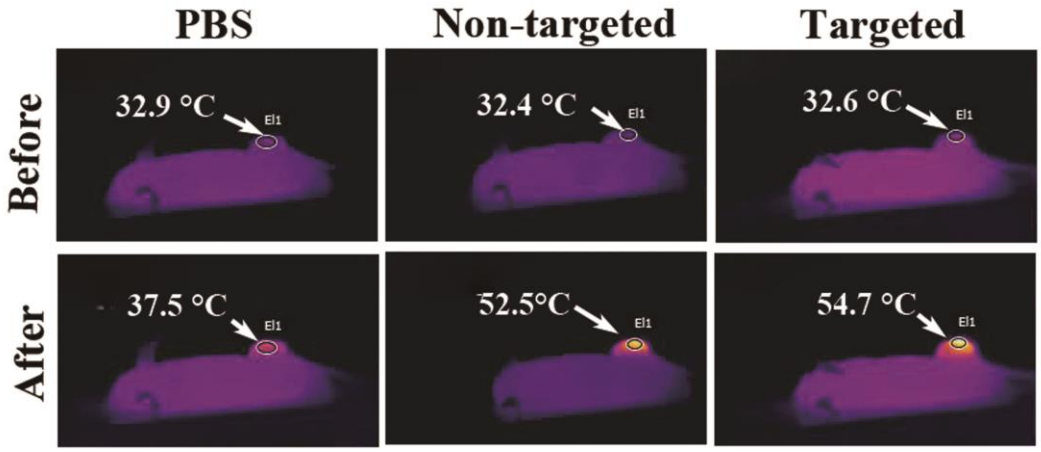

Fig. S13 In vivo thermal images of tumor before and after intratumor injection of PBS, Non-targeted and Targeted NPs ([Fe]=300 μg mL^{-1}).

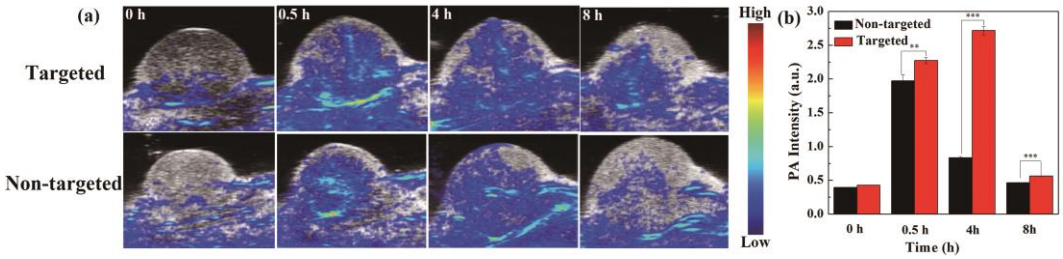

Fig.S14 (a) *In vivo* PA images and (b) the corresponding PA intensity of tumor after intratumoral injection of non-targeted and targeted NPs ([Fe]=300 μg mL^{-1}, in 0.1 mL PBS).